Supporting Information for

Solar-driven electrochemical NH_3 splitting into H_2 and N_2

Miwako Teranishi,[a] Shin-ichi Naya[a*] and Hiroaki Tada[b*]

[a] Environmental Research Laboratory, Kindai University, 3-4-1, Kowakae, Higashi-Osaka, Osaka 577-8502, Japan.

[b] Institutes of Innovation for Future Society, Nagoya University, Furo-cho, Chikusa-ku, Nagoya, Aichi 464-8603, Japan.
E-mail: shinichi.naya@itp.kindai.ac.jp, hiroaki.tada@mirai.nagoya-u.ac.jp

Table of Contents

Materials

Fluorine-doped tin(IV) oxide film-coated glass (FTO, Aldrich TEC7, sheet resistance = 7 Ω/square) and Nafion film (Nafion 117, thickness = 0.007 inch) were purchased from Aldrich. $Bi(NO_3)_3 \cdot 5H_2O$ (> 99.5%), acetic acid ($C_2H_4O_2$, > 99.7%), $VO(acac)_2$ (> 97.0%), acetylacetone (> 99.5%), $SnCl_4 \cdot 5H_2O$ (> 98.0%), EtOH (> 99.5%), Na_2SO_4 (> 99.0%), and ammonia solution (28.0-30.0%) were purchased from KANTO CHEMICAL CO., INC. All chemicals were used as received without further purification.

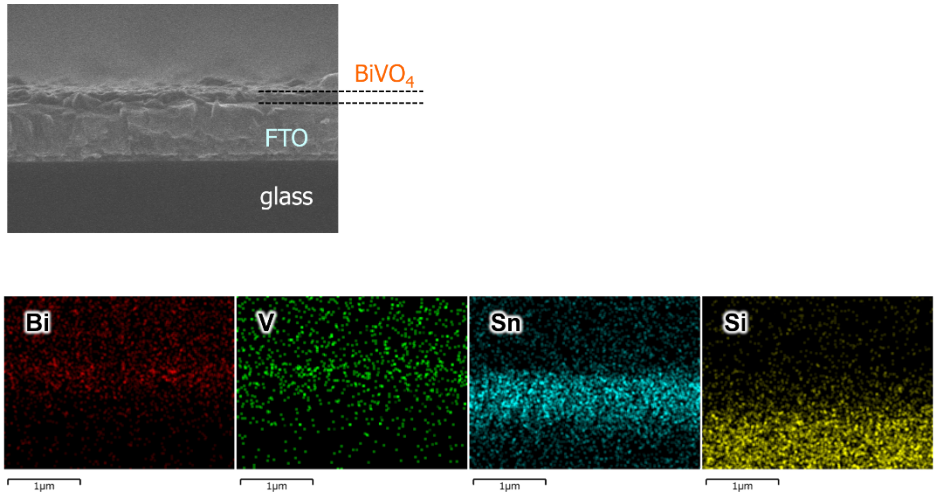

Fig. S1. SEM image (upper) and energy dispersive X-ray spectroscopy (EDS)-elemental mapping (lower) of the cross-section of $BiVO_4$(*N* = 10)/FTO.

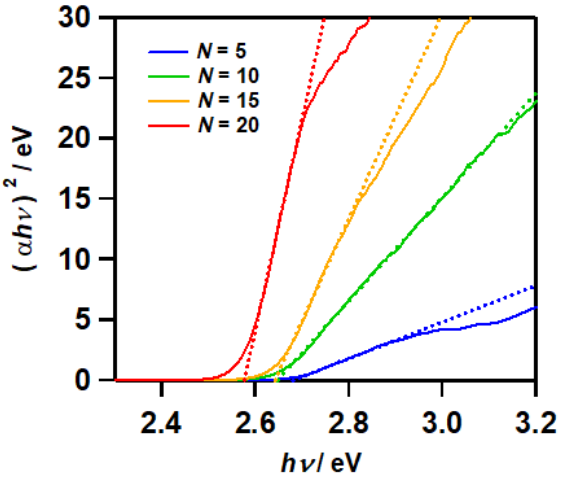

Fig. S2. Tauc plots for $BiVO_4$/FTO samples prepared by repeating the spin coating *N* times.

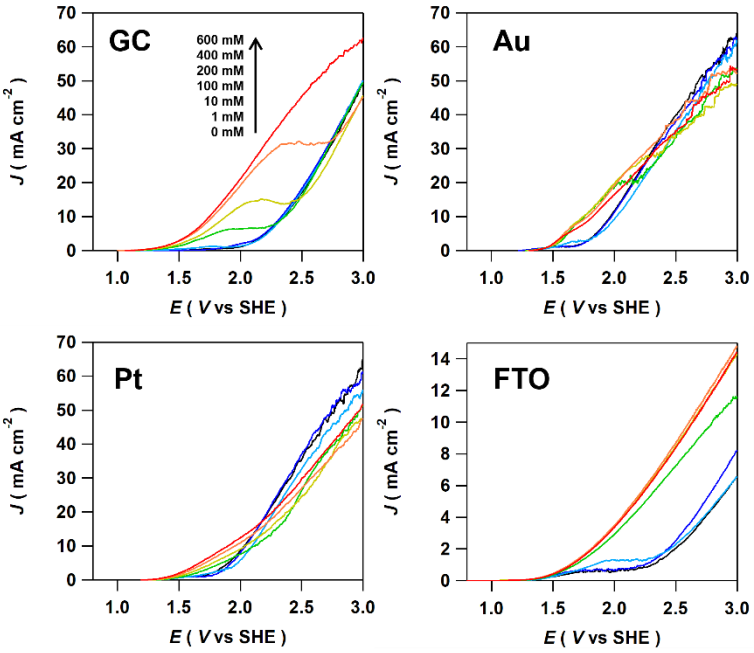

Fig. S3. Dark current-potential curves for several electrodes in deaerated 0.1 M Na_2SO_4 aq. containing NH_3 with varying concentrations pH 11.

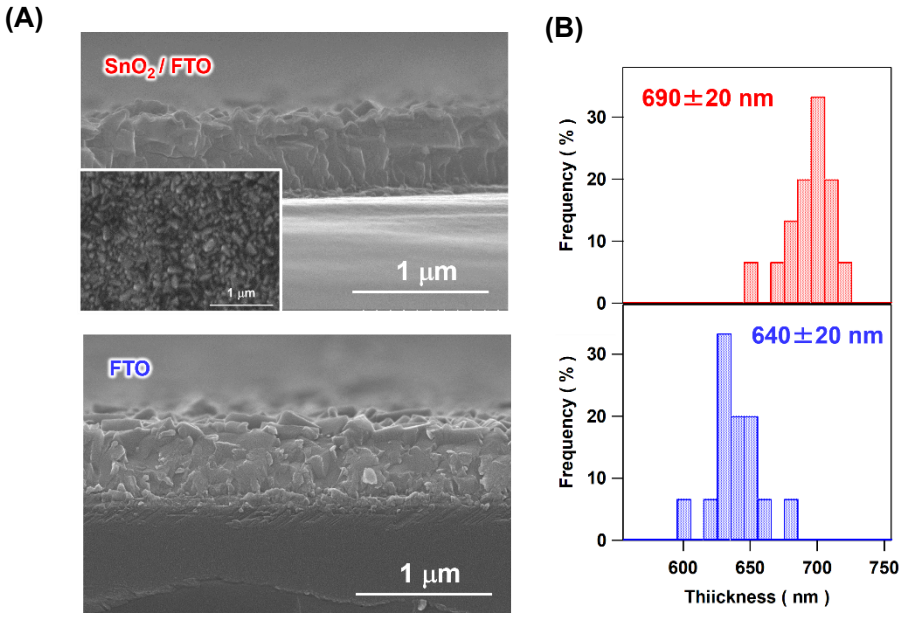

Fig. S4. (A) SEM images of the cross-sections of SnO_2/FTO (upper) and FTO (lower). The inset shows the SEM image of the SnO_2/FTO surface in the upper panel. (B) Film thickness distribution of SnO_2/FTO (upper) and FTO (lower).

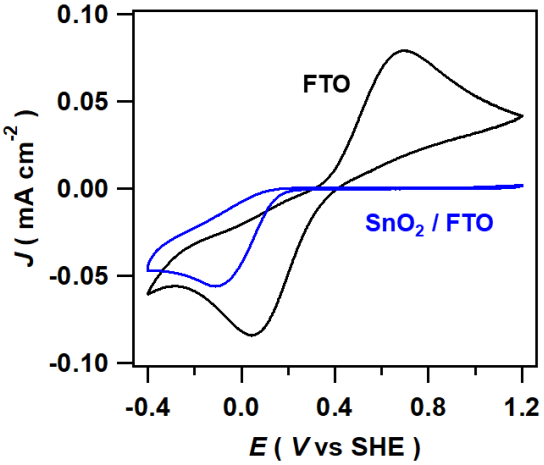

Fig. S5. CVs of FTO and SnO_2/FTO electrodes in an aqueous electrolyte solution containing $[Fe(CN)_6]^{3-}/Fe(CN)_6^{4-}$ redox pairs.

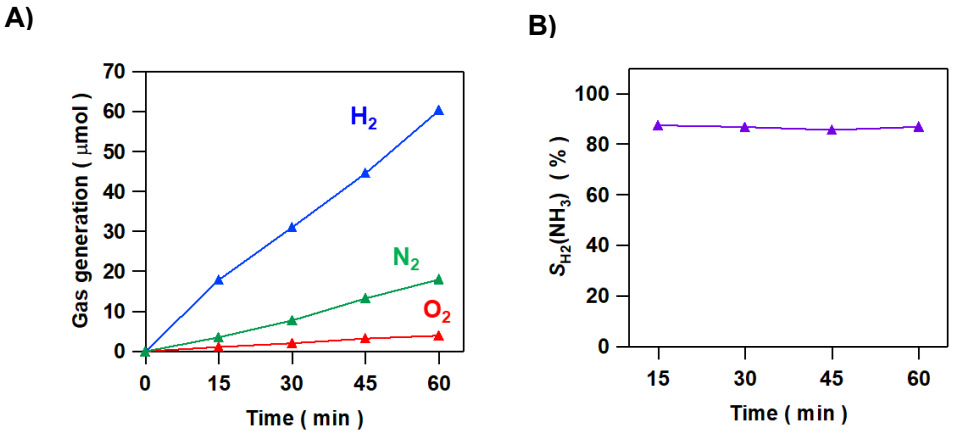

Fig. S6. (A) Product analysis in the EC reaction with the FTO electrode at E = +2.2 V in 0.1 M Na_2SO_4 electrolyte solution containing 0.59 M NH_3 (pH 11). (B) The selectivity of H_2 production from NH_3 ($S_{H2}(NH_3)$) as a function of reaction time.

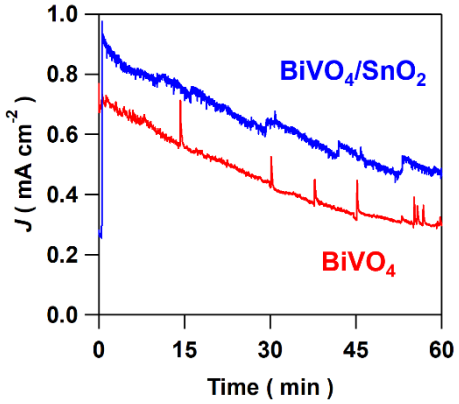

Fig. S7. PCA curves for the $BiVO_4$/FTO and $BiVO_4/SnO_2$/FTO electrodes in 0.1 M Na_2SO_4 electrolyte solution (pH 11) under illumination of visible light (λ > 430 nm) in simulated sunlight (AM 1.5, 100 mW cm^{-2}, one sun).

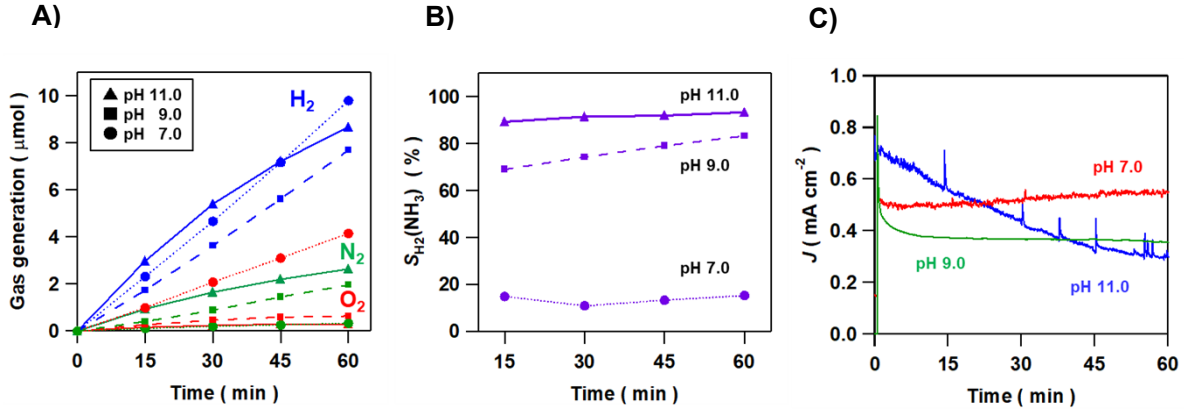

Fig. S8. pH-dependence of the PEC properties of the $BiVO_4$/FTO electrode in 0.1 M Na_2SO_4 electrolyte solution (pH 7, 9, 11) under illumination of visible light (λ > 430 nm) in simulated sunlight (AM 1.5, 100 mW cm^{-2}, one sun): (A) Product analysis (blue H_2, green N_2, red O_2), (B) Selectivity of H_2 production from NH_3 ($S_{H2}(NH_3)$), (C) PCA curves.

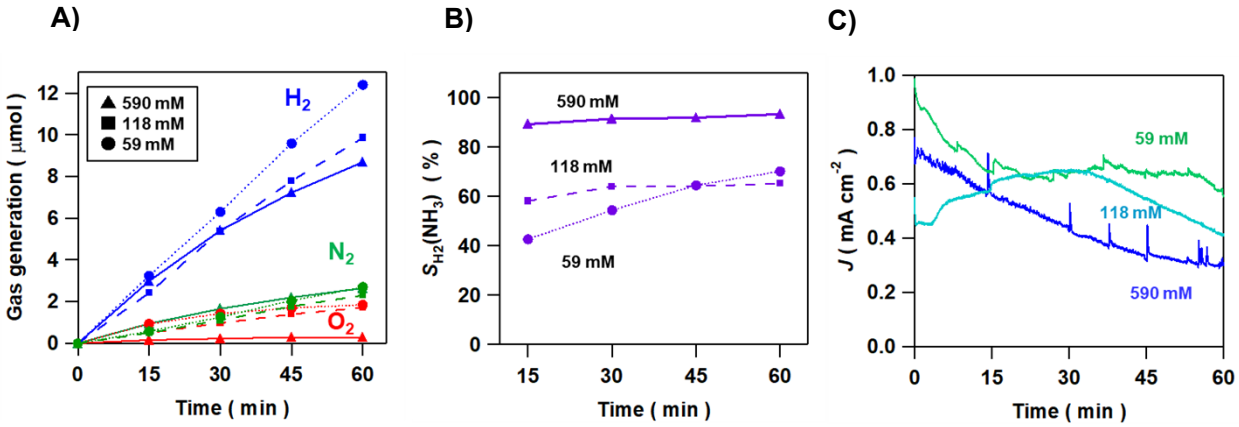

Fig. S9. NH_3 concentration-dependence of the PEC properties of the $BiVO_4$/FTO electrode in 0.1 M Na_2SO_4 electrolyte solution (pH 11) under illumination of visible light (λ > 430 nm) in simulated sunlight (AM 1.5, 100 mW cm^{-2}, one sun): (A) Product analysis (blue H_2, green N_2, red O_2), (B) Selectivity of H_2 production from NH_3 ($S_{H2}(NH_3)$), (C) PCA curves.

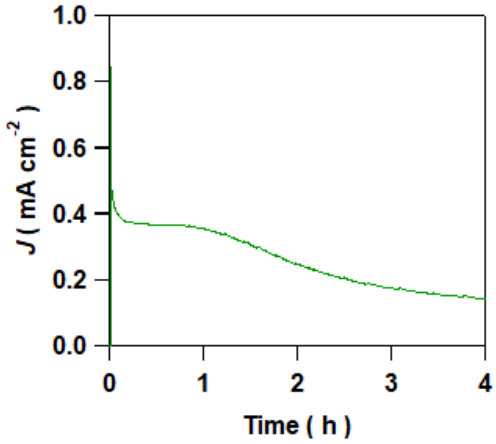

Fig. S10. Long-term stability of the $BiVO_4$/FTO electrode. The PCA curve was measured in 0.1 M Na_2SO_4 electrolyte solution containing 0.59 M NH3 (pH 9) under illumination of visible light (λ > 430 nm) in simulated sunlight (AM 1.5, 100 mW cm^{-2}, one sun).

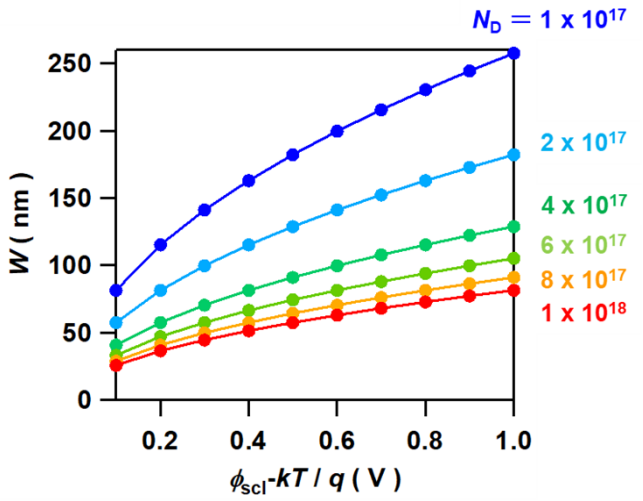

Fig. S11. Plots of width of the space charge layer (W) as a function of $\phi_{scl} - kT/q$.

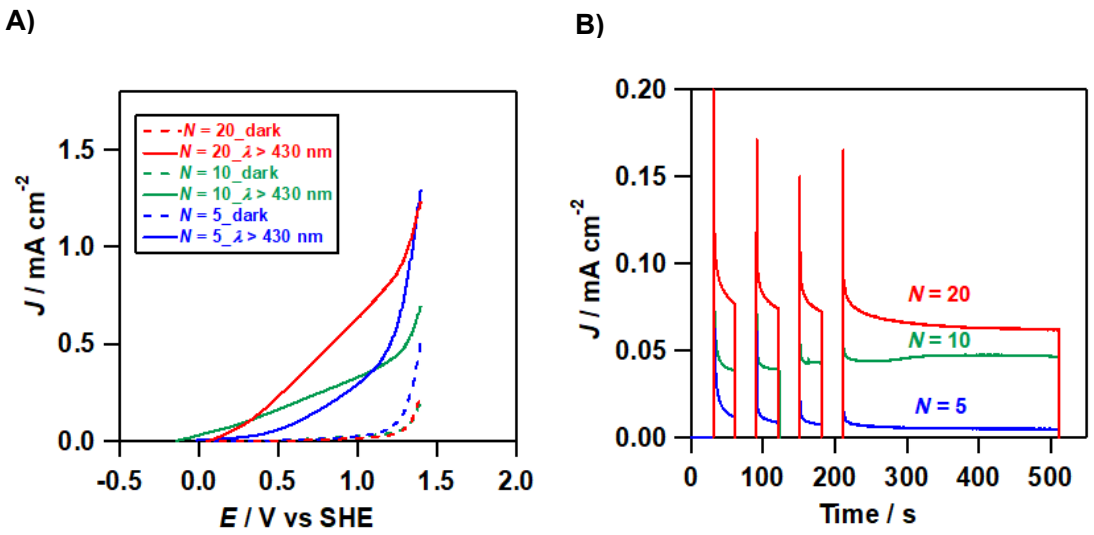

Fig. S12. (A) *J-E* curves of $BiVO_4$(*N* = 5, 10, 20)/FTO with different $BiVO_4$ film thickness in 0.1 M Na_2SO_4 electrolyte solution containing 0.59 M NH_3 (pH 11) under illumination of visible light (λ > 430 nm) in the simulated sunlight (AM 1.5, 100 mW cm^{-2}, one sun). (B) PCA curves of $BiVO_4$(*N* = 5, 10, 20)/FTO at the rest potential in the dark (*E* = +0.164 V) under the same irradiation conditions.